[10]W. H. Parker, B. N. Taylor, and D. N. Langenberg, Rev. Mod. Phys. 41, 375 (1959).
[11]S. D. Drell and J. D. Sullivan, Phys. Rev. 154, 1477 (1967).
[12]S. B. Crampton, D. Kleppner, and N. Ramsey, Phys. Rev. Lett. 11, 338 (1963).
[13]This possible effect was first mentioned to us by Dr. C. Bouchiat.
[14]G. S. Heyne and H. G. Robinson, private communication.
[15]R. M. Herman, Phys. Rev. 136A, 1576 (1964).
[16]J. F. Hague *et al.*, Phys. Rev. Lett. 25, 628 (1970).
[17]T. Fulton, D. A. Owen, and W. W. Repko, private communication.

Decisive Tests of High-Energy Models*

Edmond L. Berger and Geoffrey Fox†
High Energy Physics Division, Argonne National Laboratory, Argonne, Illinois 60439
(Received 21 September 1970)

Regge-pole and strong-absorption (diffractive) models are based upon fundamentally different physical postulates. Although both reproduce available $d\sigma/dt$ and polarization data, profound differences are evident in basic amplitude structure. We show that measurements of the spin-rotation parameters R and A, for any high-energy exchange process, will determine structure of amplitudes and thus provide unambiguous tests of essential assumptions in the models. We examine explicitly the experimentally feasible reactions $\pi N \to K(\Lambda,\Sigma)$, $\bar{K}N \to \pi(\Lambda,\Sigma)$, and $\gamma p \to K(\Lambda,\Sigma)$, as well as multiparticle processes.

In this Letter, we stress the importance of new measurements designed to determine individual helicity amplitudes. We propose a set of experiments which will decisively test models of strong interactions. These experiments are both feasible and directly interpretable.

There are profound differences between current models[1] which are not merely the result of alternative parametrizations. For example, dip-bump phenomena in $d\sigma/dt$ are interpreted in completely different ways in traditional Regge-pole theory and in the strong-cut Regge-absorption model (SCRAM).[2,3] Although both models reproduce available data on differential cross sections and polarization (P), the basic structure of helicity amplitudes differs greatly. More precise data on $d\sigma/dt$ and P will serve primarily to determine better the parameters within models. However, progress in testing underlying assumptions and in distinguishing among models demands a more complete set of experiments. In meson-nucleon scattering, measurements of the spin-rotation parameters R and A are essential.[4] It is also important to realize that structure in the R and A distributions, themselves, are unambiguously characteristic of the models. Indeed, by a simple glance at the experimental distributions for associated production, without detailed fits, one will be able to determine immediately whether assumptions underlying SCRAM are correct. As far as we are aware, this has not been pointed out before. It certainly gives great impetus to work with polarized particles.

In this note, we concentrate on reactions with hyperons in the final state; examples are $\bar{K}p \to \pi\Sigma$, $\gamma p \to K\Lambda$, $\pi p \to K\pi\Sigma$. If these are done with a polarized target (and/or with polarized photons), the weak decay of the hyperon can be used to determine the crucial spin-rotation parameters. In paragraphs which follow, we first summarize distinctive features of models which should be tested; secondly, we discuss relevant experimental observables for meson-baryon scattering; and finally, we treat photoproduction and multiparticle processes.

Models[1] are characterized by quite different positions and interpretation of zeros of amplitudes. The zeros of Regge-pole theory are the wrong-signature nonsense zeros. In the exchange degeneracy form of the Regge-pole theory, these occur when the signature factor $(1 \pm e^{-i\pi\alpha})$ vanishes—i.e., at values of t such that the trajectory function $\alpha(t) = 0, -2, \cdots$ (odd signature), or -1, $-3, \cdots$ (even signature). We emphasize that (i) the location of a given zero is the same in all spin amplitudes; (ii) the location is determined by the trajectory function and signature of the exchanged particle, and thus it will occur at different values of t for processes dominated by different trajectories; (iii) the real part of the amplitude has double zeros at $1 \pm \cos\pi\alpha = 0$, whereas the imaginary part has single zeros at $\sin\pi\alpha = 0$. By contrast, (i) the zeros of SCRAM[2]

are not correlated at all with the trajectory function or signature; (ii) the locations of zeros are the property of the spin amplitudes, e.g., for all reactions,[5] for helicity nonflip the zero is at $t \approx -0.2$ (GeV/c)^2, and for single-flip amplitudes the zero is at $t \approx -0.6$ (GeV/c)^2; (iii) both real and imaginary parts of amplitudes have the same (single) zero structure.

At present, there are only a few features of data which test the zero structure of models. Evidence from $d\sigma/dt$, P, and finite energy sum rules is indirect and ambiguous. A zero in the imaginary part of the ρ nonflip amplitude near $t \approx -0.2$ (GeV/c)^2 is established through the crossover effect in $\pi^{\pm}p d\sigma/dt$. This is a success for SCRAM and, correspondingly, a difficulty for pole models. On the other hand, if we assume that the Pomeranchukon is purely imaginary, measurements of polarization in pp, $\bar{p}p$, $K^{\pm}p$, and $\pi^{\pm}p$ elastic scattering[6] are in agreement with the t dependence predicted by the signature factor of ρ and A_2 Regge-pole models. In SCRAM, the same assumption leads to the incorrect prediction of a change of sign in polarization for all elastic precesses at $t \approx -0.6$ (GeV/c)^2. This and other evidence suggests a curious picture in which the pattern of zeros agrees best with SCRAM expectations for the imaginary part, but with the Regge-pole model for the real part of amplitudes. Fortunately, as we now discuss, determination of R and A will resolve these ambiguities.

Meson-baryon scattering.—We begin by displaying amplitudes obtained from fits[7] to meson-nucleon data with traditional Regge-pole theory and with SCRAM. For definiteness, we show results for $\bar{K}N \to \pi\Sigma$; however, these amplitudes, in fact, are typical of a wide class of exchange processes. We use s-channel helicity amplitudes H_{++} and H_{+-}, normalized so that

$$d\sigma/dt = |H_{++}|^2 + |H_{+-}|^2 \text{ mb/(GeV/}c)^2. \quad (1)$$

In Figs. 1(a) and 1(c), real and imaginary parts of the SCRAM spin-nonflip H_{++} and spin-flip H_{+-} amplitudes are shown. Corresponding quantities from the exchange-degenerate (EXD) Regge pole fit are given in Figs. 1(b) and 1(d). The EXD Regge-pole amplitudes are purely real; however, that fact is not important per se. As described above, the pattern of the zeros in amplitudes is the essential difference between the SCRAM and pole models. Indeed, as shown in the figure, the SCRAM amplitudes H_{++} and H_{+-} are zero near $t = -0.2$ and $t = -0.6$ (GeV/c)^2, respectively.

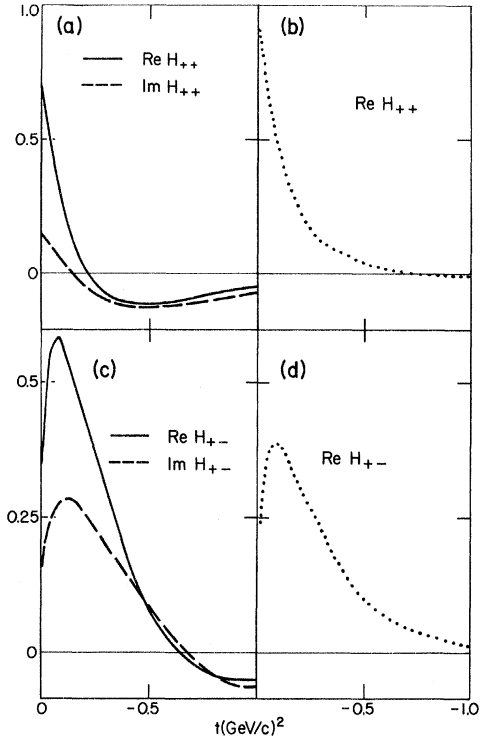

FIG. 1. Amplitudes (Ref. 7) for $K^-p \to \pi^-\Sigma^+$ at 4.07 GeV/c. (a), (c) Real and imaginary parts of H_{++} and H_{+-}, respectively, for the SCRAM model; (b), (d) ReH_{++} and ReH_{+-} for the EXD Regge-pole model.

This property is not shared by the Regge-pole amplitudes.

There are experimental quantities which reflect directly the presence of absence of structure in the basic amplitudes. These are the spin-rotation parameters $\hat{R}$ and $\hat{A}$, which we define as

$$\hat{R} = 2\,\mathrm{Re}(H_{++}H_{+-}^*)/(|H_{++}|^2 + |H_{+-}|^2), \quad (2)$$

$$\hat{A} = (|H_{++}|^2 - |H_{+-}|^2)/(|H_{++}|^2 + |H_{+-}|^2). \quad (3)$$

At high energy these are essentially equal to the corresponding traditional[4] quantities R and A, given by $R = \hat{R}\cos\theta_s - \hat{A}\sin\theta_s$ and $A = \hat{R}\sin\theta_s + \hat{A} \times \cos\theta_s$, where θ_s is the s-channel c.m. scattering angle. For completeness, here, we note also that

$$P = 2\,\mathrm{Im}(H_{++}H_{+-}^*)/(|H_{++}|^2 + |H_{+-}|^2). \quad (4)$$

In Figs. 2(a), 2(c), and 2(e) we show values of P, R, and A for $K^-p \to \pi^-\Sigma^+$ at 4.07 GeV/c. These curves are obtained from the amplitudes given in Fig. 1. We note that the Regge-pole

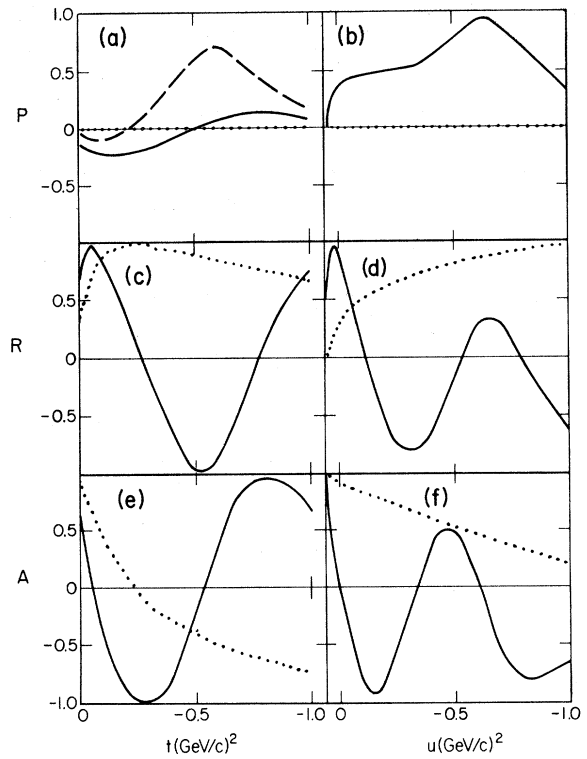

FIG. 2. Observables (a) P, (c) R, and (e) A for $\bar{K}N \to \Sigma\pi$ at 4.07 GeV/c; (b) P, (d) R, and (f) A for $\pi^- p$ backward elastic at 9.85 GeV/c. The dotted line comes from a Regge-pole model [Ref. 7 for (a), (c), and (e) and Ref. 10 for (b), (d), and (f)]. The solid line is the prediction of SCRAM [Ref. 7 for (a), (c), and (e) and Ref. 3 for (b), (d), and (f)]. The dashed line in (a) is the SCRAM prediction for $\pi N \to K\Sigma$ at 14 GeV/c; R and A distributions for $\pi N \to K\Sigma$ are essentially identical to those given for $\bar{K}N \to \pi\Sigma$.

model gives singularly featureless distributions in R and A; by contrast, SCRAM provides dramatic structure near both $t = -0.2$ and $t = -0.6$ (GeV/c)^2. Simple inspection of Eqs. (2) and (3), together with the amplitudes of Fig. 1, shows clearly that structure in R and A reflects precisely the canonical zero pattern of SCRAM amplitudes. By contrast, P and $d\sigma/dt$ are fairly smooth and give little hint of the activity in the underlying amplitudes. As indicated by Eqs. (2) and (3), the SCRAM structure shown in R and A distributions for $K^- p \to \pi^- \Sigma^+$ is actually a general feature of all exchange processes. For example, structure in R (and A) is essentially identical for both $\pi^+ p \to K^+ \Sigma^+$ and $K^- p \to \pi^- \Sigma^+$, whereas polarizations differ substantially [see Fig. 2(a)]. The generality of our results is illustrated further in Figs. 2(b), 2(d), and 2(f). These latter curves pertain to $\pi^- p$ backward elastic scattering at 9.85 GeV/c.[8] For both the pole model and SCRAM, we note that structure in the R and A curves is quite similar in both $\pi^- p$ backward elastic and forward $\bar{K}N \to \pi\Sigma$, even though the exchanges in these two reactions are quite different. Again, in SCRAM, the magnitude and structure of R and A are an immediate consequence of the postulated pattern of zeros in SCRAM amplitudes; on the other hand, P is sensitive to small parameter variation and could be very much smaller than the curve we show in Fig. 2(b), without significant changes in R and A.[3]

We recommend that high priority be given to a precise measurement of all observables ($d\sigma/dt$, P, R, and A), as a function of t, for any meson-baryon exchange process, at an energy of 5 GeV/c or greater.

Discussion and other applications of R- and A-type measurements.—We generalize our results somewhat and then treat photoproduction and multiparticle processes. First, we note that Eqs. (2) and (6) show that $\hat{R}$ and P are the real and imaginary parts of the same quantity. All present models predict both spin amplitudes to have essentially the same phase near $t = 0$; thus, to first approximation, R is maximal (for given sizes of the two-spin amplitudes) and P is zero [compare Figs. 2(a) and 2(c)]. Correspondingly, R tests the dominant features, and P the small corrections to models. This is the basic reason why R is so much more valuable than P for testing models. Not only in meson-baryon scattering, but in other processes, as well, it is particularly valuable to measure observables which correspond to real parts of bilinear products of amplitudes. These observables include the x and z components of final baryon polarization for scattering from a polarized target. In the helicity frame, with relevant factors removed,[9] we denote these by T_x and T_z, if the target is polarized perpendicular to the beam, and by L_x and L_z, if the target is polarized along the beam. For the simple case of meson-baryon scattering, $T_x = L_z = \hat{A}$ and $T_z = L_x = \hat{R}$. In any process the equalities $T_x = L_z$ and $T_z = L_x$ follow from the presence of only natural-parity exchange. More generally, the four quantities carry independent information.

In a Regge-pole model, factorization of pole residues predicts that each of these four quantities is essentially the same in all reactions dominated by a given Regge trajectory. By contrast, in SCRAM, L_x, L_z, T_x, and T_z are characteristic of s-channel spin structure, not of the exchange quantum numbers. We illustrate these differences with our fits to $\gamma N \to K\Sigma$. We have obtained

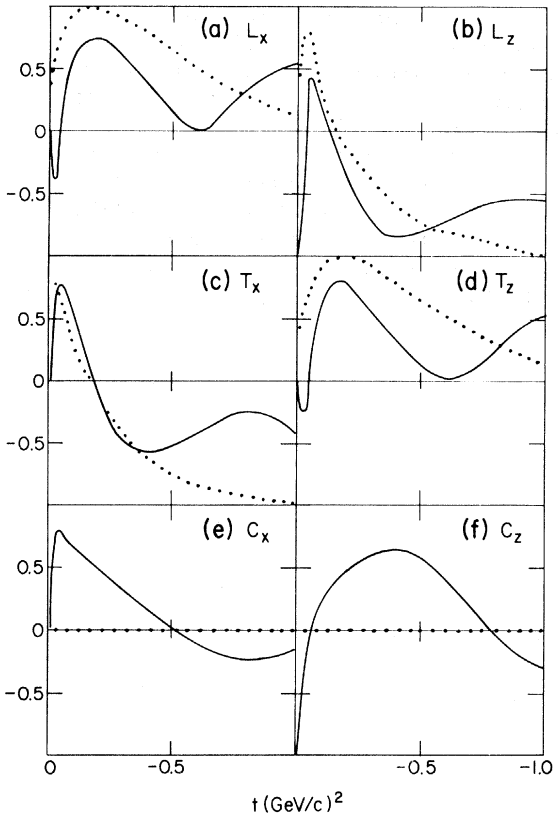

FIG. 3. Observables for $\gamma p \to K\Sigma$ at 16 GeV/c. The dotted line is the pole-model prediction and the solid line is the SCRAM result.

Regge-pole model and strong-absorption model fits to all available data on $\gamma N \to KY$. We include contributions of K, K^*, and K^{**} exchanges. Above 5 GeV/c, however, data are dominated by the K^* and K^{**} trajectories, the same trajectories which mediate $\pi N \to KY$ and $KN \to \pi Y$, discussed above. In Figs. 3(a)-3(d), we give L_x, L_z, T_x, and T_z from both our pole model and our SCRAM fits. By comparing Fig. 2(c) with Figs. 3(a) and 3(d), or Fig. 2(e) with Figs. 3(b) and 3(c), one sees clearly that, as expected, the pole model predicts essentially the same distributions in both photoproduction and meson-baryon scattering. For SCRAM, however, the corresponding distributions differ greatly. It would be striking evidence for SCRAM and against factorization if, indeed, T_x and T_z should be so different in meson-baryon and in photoproduction processes.

Differences between SCRAM and the pole model are exhibited clearly in the final-baryon polarization for an experiment with circularly polarized photons (unpolarized target). We denote these observables[9] by C_x and C_z; they are, again, real parts of bilinear products of amplitudes. The pole model predicts $C_x = 0$ and $C_z = 0$. For SCRAM curves, the structure shown in Figs. 3(e) and 3(f) reflects the distinctively different absorption effects in the spin-nonflip and double-flip amplitudes.

As a final example, we emphasize the novel importance of R- and A-type measurements in multiparticle processes. We imagine $(\pi, \bar{K})N \to \mathrm{MM} + Y$ in a kinematic region such that it can be interpreted in terms of the exchange of some trajectory at the $N\bar{Y}$ vertex. In the pole model, factorization predicts the same ratio of spin flip to spin nonflip at the $N\bar{Y}$ vertex as in two-body data. Just as in photoproduction, this assertion may be tested by examining L_x, L_z, T_x, and T_z, discussed above. Furthermore, important new information is now carried by the y component of final-baryon polarization. This observable contains a term which measures directly the amounts of natural- and unnatural-parity exchange, entirely independently of whatever system of particles (MM) is produced in the final state, along with Y.

In summary, then, we have shown that a new class of feasible experiments, at energies of 5 GeV/c and above, will provide crucial new insight into strong-interaction phenomena and resolve decisively outstanding ambiguities among existing phenomenological models.

We are grateful to Chris Quigg for critical comments. Our attention was drawn to the possible importance of R and A measurements by Frank Pipkin and Aki Yokosawa at the National Accelerator Laboratory Summer Study.

---

*Work supported by the U. S. Atomic Energy Commission.

†Present address: California Institute of Technology, Pasadena, California.

[1]Recent reviews of high-energy models include L. Durand, III, in *Proceedings of the International Conference on Expectations for Particle Reactions at the New Accelerators, April 1970* (Univ. of Wisconsin-Madison, 1970); G. C. Fox, in *Proceedings of the Third International Conference on High-Energy Collisions, Stony Brook, 1966,* edited by G. C. Fox (Gordon and Breach, New York, 1969); J. D. Jackson, Rev. Mod. Phys. 42, 12 (1970).

[2]M. Ross, F. S. Henyey, and G. L. Kane, to be published.

[3]For an explicit comparison of sundry models for πN backward scattering see E. L. Berger and G. C. Fox, ANL Report No. ANL/HEP 7019 (unpublished).

[4]For discussions of R, A, and more general spin-

rotation parameters see L. Wolfenstein, Phys. Rev. 96, 1654 (1954); A. Białas and B. E. Y. Svensson, Nuovo Cimento A42, 908 (1966); J. D. Jackson, in *Proceedings of the International Conference on Polarized Targets and Ion Sources, Saclay, 1966* (Centre d'Etudes Nucléaires de Saclay, Saclay, France, 1967), p. 3; M. Jacob, *ibid.*, p. 235; R. J. N. Phillips, *ibid.*, p. 273.

[5]For a complete treatment, including cases for which the input Regge-pole amplitude vanishes at $t=0$, see Ref. 2.

[6]G. Belletini, "Polarization in Elastic Scattering at High Energy" (to be published).

[7]These fits were done in collaboration with Chris Quigg. Details will be reported elsewhere. All available $d\sigma/dt$ and P data were incorporated in the fits.

[8]Measurement of R and A for $\pi^- p \to p\pi^-$ at high energy is technically impossible at present. The predictions for backward $K^- p \to \Sigma^+ \pi^-$ are, however, identical to Figs. 2(b), 2(d), and 2(f).

[9]Explicit definitions of these observables as well as of all other observables in photoproduction processes is given in E. L. Berger and G. C. Fox, ANL Report No. ANL/HEP 7023 (unpublished). This report also contains a more detailed discussion of many points raised in this Letter. We would be glad to supply any interested reader with predictions of our models. A detailed article is also in preparation.

[10]V. Barger and D. Cline, Phys. Rev. Lett. 21, 392 (1968).

ERRATUM

RESONANT CANCELATION OF RAMAN SCATTERING FROM CdS AND Si. J. M. Ralston, R. L. Wadsack, and R. K. Chang [Phys. Rev. Lett. 25, 814 (1970)].

Equation (3) should be written

$$\frac{S_{\mathrm{CdS}}^{\mathrm{TO}}}{S_{\mathrm{CS_2}}} = [\pm Af(\omega_c - \omega_1) + B]^2.$$